

Nuclear resonant scattering of synchrotron radiation by ^{187}Os D. Bessas,^{1,*} I. Sergueev,² D. G. Merkel,¹ A. I. Chumakov,¹ R. Rüffer,¹ A. Jafari,^{1,3,4} S. Kishimoto,⁵ J. A. Wolny,⁶ V. Schünemann,⁶ R. J. Needham,⁷ P. J. Sadler,⁷ and R. P. Hermann^{3,4,†}¹European Synchrotron Radiation Facility, F-38043 Grenoble, France²Deutsches Elektronen-Synchrotron, D-22607 Hamburg, Germany³Jülich Centre for Neutron Science, JCNS, and Peter Grünberg Institut PGI, JARA-FIT,

Forschungszentrum Jülich GmbH, D-52425 Jülich, Germany

⁴Faculté des Sciences, Université de Liège, B-4000 Liège, Belgium⁵Institute of Materials Structure Science, KEK, 1-1 Oho, Tsukuba, Ibaraki 305-0801, Japan⁶Technische Universität Kaiserslautern, Fachbereich Physik, D-67663 Kaiserslautern, Germany⁷Department of Chemistry, University of Warwick, Coventry CV4 7 AL, United Kingdom

(Received 3 April 2015; revised manuscript received 7 May 2015; published 11 June 2015)

We performed nuclear forward and inelastic scattering of synchrotron radiation by elemental Os utilizing the nuclear excited state of ^{187}Os which is otherwise inaccessible using any practical radioactive decay process. The lifetime of the excited state, 3.06(8) ns, and the energy of the transition, 9.778(3) keV, are refined. The nuclear quadrupole moment of the excited state, $Q_{3/2} = 1.46(10)$ b, is determined. The density of phonon states for elemental Os, which is herein experimentally determined, suggests that the Os lattice is a model for the lattice dynamics of hcp-Fe. The combination of the low energy of the nuclear transition and the large nuclear mass leads to a high recoil free fraction, $f_{LM} = 0.95(1)$, at room temperature, a large value that strongly supports the viability of nuclear resonance scattering as a reliable method to study electronic, magnetic, and elastic properties of Os compounds, including Os organometallics.

DOI: [10.1103/PhysRevB.91.224102](https://doi.org/10.1103/PhysRevB.91.224102)

PACS number(s): 76.80.+y, 41.85.Si, 75.50.Cc, 76.20.+q

I. INTRODUCTION

Along with its congeners iron and ruthenium, osmium is a group-8 transition metal. It stands among the compounds with the highest density, 22.59 g/cm³, and melting point, 3306 K [1] and crystallizes in a hexagonal structure with symmetry $P63/mmc$. In the metallic state Os has mainly drawn scientific interest because of its unexpectedly high bulk modulus [2], which is comparable to the bulk modulus in the covalently bonded carbon in diamond, and because of a debated electronic topological transition around 25 GPa [3].

No less than 11 oxidation states have been observed for osmium in compounds or complexes, and within the majority of them it appears in octahedral coordination [4]. Studies of the hyperfine interactions between the Os nuclei and the host environment may provide information on the electronic properties of Os compounds via the determination of the isomer shift, the electric field gradient, as well as the magnetic hyperfine field. Direct experimental techniques such as nuclear magnetic resonance (NMR) or Mössbauer spectroscopy can in principle be used as a local probe to obtain this information. However, there are only two NMR active isotopes for Os, namely ^{187}Os and ^{189}Os . The NMR signal from ^{187}Os is difficult to observe because of its low nuclear magnetic moment. The ^{189}Os nucleus has a quadrupole moment in its ground state and yields very broad nuclear magnetic resonances. Thus, currently only indirect NMR detection of Os via proton coupling is carried out [5]. The same Os isotopes are the most favorable energywise for performing

Mössbauer spectroscopy. Mössbauer spectra using ^{189}Os have been successfully measured by both the 36.2- and the 69.5-keV nuclear transitions by Wagner *et al.* [6]. The short half-life of the radioactive source of only 13 days makes such studies impractical for the broader scientific community. Mössbauer spectroscopy using ^{187}Os is inapplicable because no practical radioactive source for this isotope exists.

The lattice dynamics in Os compounds is interesting mainly because Os is isoelectronic in its valence d electrons with Fe. In this respect the lattice dynamics and the functional properties in fields like thermoelectricity [7,8], magnetism [9], and superconductivity [10] can be tailored. Moreover, the elastic properties of elemental Os are particularly interesting because Os is a possible model for ε -Fe (hcp) in studies related to conditions in the Earth's interior [11,12]. More importantly, lately Os organometallic complexes have been reported to have medical applications [13]. Knowledge of the lattice dynamics in such compounds may help to correlate the differences in the interatomic bonding with respect to the functionality of these compounds.

In this study, we pave the way for lattice dynamical and hyperfine characterization studies in Os compounds by nuclear forward scattering (NFS) [14,15] and nuclear inelastic scattering (NIS) [16,17] using the low-lying nuclear level at 9.78 keV of ^{187}Os . From our NFS data we were able to determine the previously unknown nuclear quadrupole moment of the first excited state. By utilizing a monochromator with 1-meV bandpass we collected high quality NIS spectra. We present the experimentally obtained density of phonon states (DOS) of elemental Os and we provide feedback for refining the Os potential in first-principle theoretical calculations for osmium compounds. Comparison with the corresponding DOS in the high-pressure, hcp, ε -Fe phase indicates that ambient condition Os is a model of Fe at high pressure. We further suggest that

*bessas@esrf.fr

†Present address: Materials Science and Technology Division, Oak Ridge National Laboratory, Oak Ridge, Tennessee 37831, USA.

both nuclear forward and inelastic scattering spectroscopy are strong candidates to become the major hyperfine and lattice dynamical characterization techniques for osmium compounds.

II. EXPERIMENTAL METHODS

The natural abundance of ^{187}Os is $\sim 2\%$. The nuclear spin of ^{187}Os is $1/2$ in the ground state and $3/2$ in the first excited state [18]. The nuclear quadrupole moment of the ground state, $Q_{1/2}$, is 0 and for the first excited state, $Q_{3/2}$, is unknown. The nuclear transition between the first excited state and the ground state of ^{187}Os with transition energy of 9.78 keV is mainly of magnetic dipole, $M1$, origin. The mixing ratio with the electric quadrupole, $E2$, is less than 0.04 [18]. The recoil energy is very small, 0.274 meV, and makes possible NIS investigations of most Os-based materials at ambient temperature. The high internal conversion, with coefficient 280 [18], results in sizeable delayed incoherent Os M_α fluorescence at 1.921 keV that is difficult to detect due to absorption in the sample.

The experiment was carried out at the Nuclear Resonance beamline ID18 [19] of the European Synchrotron Radiation Facility. The storage ring was operating in 16-bunch mode providing x-ray flashes every 176 ns. The optical elements in the experimental setup were a Si (1 1 1) high heat load monochromator (HHLM) [20] and a dedicated high-resolution monochromator (HRM); see Fig. 1(a).

The sample, 7 mg of irregularly shaped polycrystalline ^{187}Os grains with size distribution between 5 and 50 μm and 98% enrichment, was distributed in an area of 10 mm^2 and enclosed in Kapton tape. For both the NIS and NFS spectra only the 9.78-keV radiation was monitored using avalanche photo diodes (APDs) [21].

The nuclear transition energy was determined using the Si (1 1 1) HHLM. We measured the incoherent radiation from the sample using a $10 \times 10 \text{ mm}^2$, 100- μm -thick APD placed 50 mm away from the sample in horizontal scattering geometry. The energy E_0 of the nuclear transition was found to be 9.778(3) keV, with calibration to the Zn K edge at 9.660 76(3) keV [22] close to the nuclear resonance energy of ^{187}Os , and the ^{57}Fe nuclear resonance energy at 14.412 497(3) keV [23]. The energy of the transition was independently checked versus the Er-L1 at 9.7578(11) keV [24] and the Ta-L3 at 9.8767(12) keV [24] x-ray-absorption edges and was found to be 9.7768(12) keV. The value of the transition energy extracted in this study is in agreement with the previously reported value, 9.756(19) keV [18] but more accurate by an order of magnitude.

The design of a high-resolution monochromator with at least 1-meV energy resolution is challenging for energies below 10 keV [25,26] because the intrinsic Darwin width of the highest-order reflections is relatively large, e.g., a single Si(8 2 2) reflection has an energy width of 23 meV at 9.78 keV. For the high-resolution monochromator used in this study the Yabashi *et al.* [27] scheme is adopted. We used two pairs of asymmetrically cut crystals both utilizing the Si(8 2 2) reflection ($\theta_B = 82.11^\circ$ at 9.78 keV) in a (+ - - +) geometry. The asymmetry parameter, $|b| = \left| \frac{\sin(\theta_B - a)}{\sin(\theta_B + a)} \right|$ where a is the angle between the surface and θ_B is the Bragg angle, for the first pair is 0.198 and for the second pair is $1/0.198 = 5.050$. The

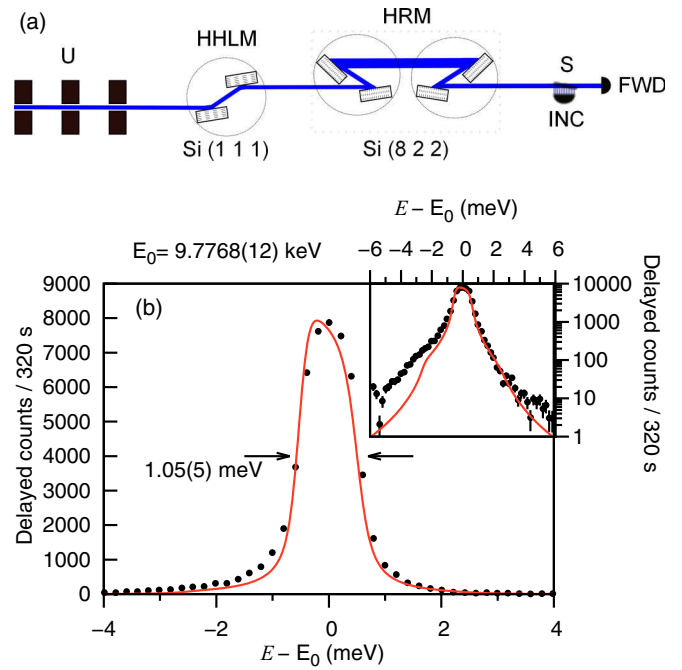


FIG. 1. (Color online) (a) The experimental setup consisted of three undulators (U), a Si (1 1 1) high heat load monochromator (HHLM), a dedicated Si (8 2 2) high-resolution monochromator (HRM) for scanning the energy, a sample (S) at ambient conditions, a Si APD for measuring the incoherent radiation (INC) and three-stacked Si APD for measuring the nuclear forward scattering (FWD). (b) The energy bandpass of the Si (8 2 2) HRM measured by the FWD detector (black points) in linear scale compared with the theoretically calculated energy response function (red line). Inset: the same data in logarithmic scale.

obtained photon flux after the HRM is $2.8 \times 10^9 \text{ ph/s/meV}$ at 90-mA storage ring electron current.

III. RESULTS AND DISCUSSION

The obtained HRM instrumental function is shown in Fig. 1(b) together with the theoretical reflectivity calculated for a 10- μrad divergent x-ray beam impinging on the monochromator. The obtained full width at half maximum is 1.05(5) meV. The tails are narrow and decrease by nearly four orders of magnitude within 6 meV. The experimental data are in agreement with the theoretical calculations. A slight discrepancy observed between the experimental data and the theoretical calculations shown in logarithmic scale, see inset to Fig. 1(b), might be related with either the misalignment of the HRM or the quality of the crystals at the surface.

The time distribution of the incoherent spectrum was measured between 10 and 40 ns, see Fig. 2(a), and reveals an exponential decay. The fit of the data with a simple exponential function, $I(t) = I_0 e^{-t/\tau_0}$, where τ_0 is the lifetime of the excited state yields a lifetime of 3.06(8) ns close to the tabulated value of 3.43(25) ns [18].

The NFS data were measured between 7 and 40 ns, see Fig. 2(b), with a count rate of 30 Hz. The NFS data show clear oscillations in addition to the usual exponential decay which stem from the electric hyperfine interaction. The electric-field

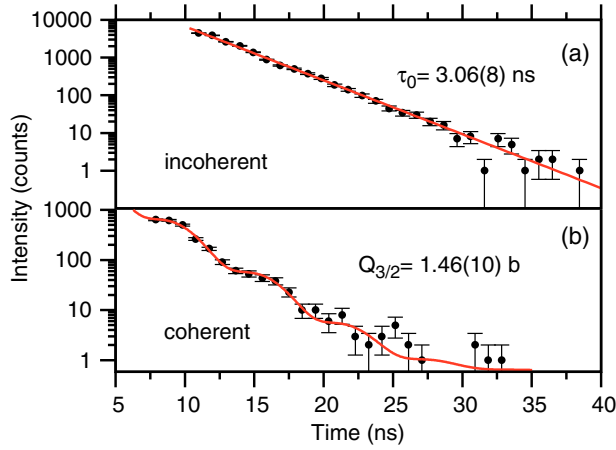


FIG. 2. (Color online) (a) The time distribution of the delayed incoherent scattering obtained on resonance by ^{187}Os metal (black points) and the fit between 10 and 40 ns using an exponential decay (red line) to obtain the lifetime of the excited state, τ_0 ; see text. (b) The time distribution of the delayed coherent scattering obtained on the same sample and the corresponding fit to obtain the nuclear quadrupole splitting, $Q_{3/2}$; see text.

gradient eq in osmium, $eq = 0.89(8) \times 10^{18} \text{ V/cm}^2$, was measured by Wagner *et al.* [6]. However, the nuclear quadrupole moment of the excited state, $Q_{3/2}$, is unknown. The small effective thickness [28] of the sample, $\xi = 0.34(11)$, allows us to fit the data with a simple analytical expression:

$$I(t) \propto \exp\left(-\left(1 + \xi/2\right)\frac{t}{\tau_0}\right) \left[1 + K \cos\left(\frac{\Delta E_Q}{\Gamma_0} \frac{t}{\tau_0} + \varphi\right)\right], \quad (1)$$

where $\Delta E_Q = (e/2) \cdot eq \cdot Q_{3/2}$ is the quadrupole splitting, e is the absolute value of the electron charge, $\Gamma_0 = 0.217(6) \mu\text{eV}$ is the natural linewidth, K is related to the grain size distribution, and φ denotes the shift of the beats due to the effective thickness. A similar equation was used to analyze NFS spectra [15] utilizing the corresponding $1/2 \rightarrow 3/2$ nuclear transition in ^{57}Fe .

The NFS spectrum shown in Fig. 2(b) is fitted between 7 and 25 ns with the formula given by Eq. (1) and the obtained value of the quadrupole splitting is $\Delta E_Q = 0.65(4) \mu\text{eV}$. Notably the observed oscillations are resolvable because the quadrupole splitting is larger than the natural linewidth, $3.0(2)\Gamma_0$, and allows us to calculate the nuclear quadrupole moment of the excited state $Q_{3/2} = 1.46(10) \text{ b}$.

The NIS spectra of Os metal were recorded at 295 K in 8 h between -20 and 35 meV with respect to the ^{187}Os transition energy. It is evident from the exponential decay that extending the measurement of the incoherent spectra to earlier time than 10 ns would allow a significant increase in the obtained count rate. The development within reach of a faster detection scheme starting at 1 ns would allow ten times faster acquisition, i.e., the NIS spectra in this study would be collected within less than an hour.

The DOS, $g(E)$, for Os, see Fig. 3, was obtained by employing the double Fourier transformation as implemented in the software DOS [29]. The Os DOS shows a Debye-like

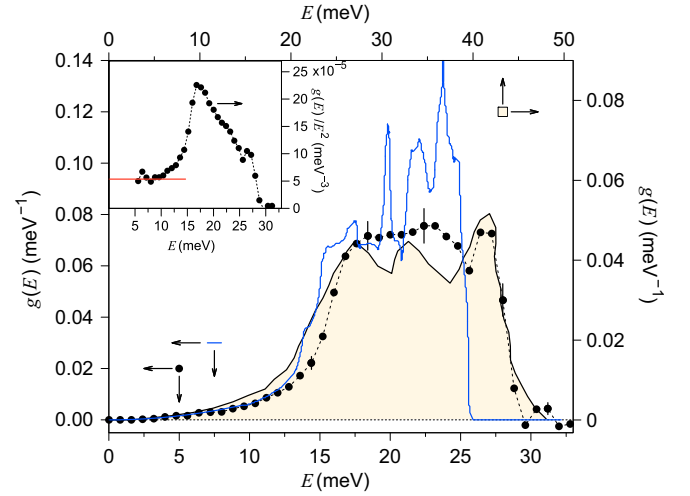


FIG. 3. (Color online) Os density of phonon states measured using nuclear inelastic scattering (black points) at 295 K; for clarity a dashed line connects the points and typical error bars are given. The theoretically calculated density of phonon states obtained by Ref. [30] (blue line). The density of phonon states of $\epsilon\text{-Fe}$ at 25 GPa obtained by Mao *et al.* [39] (yellow area and black line). Inset: The Debye level calculated between 5 and 11 meV (red line) from the data in the Debye representation.

behavior up to 11 meV. A clear peak is observed between 26 and 27 meV followed by a sharp cutoff at 28 meV.

Several first-principle calculations on the lattice dynamics of elemental Os exist in the literature [30–34] in relation with the thermodynamic properties and the existence of an electronic topological transition around 25 GPa [3]. The experimental DOS obtained herein at 295 K is compared with the *ab initio* theoretical calculations by Ma *et al.* [30]. The shape of the experimental DOS is reproduced by the theory, however, the energy axis of the theoretically calculated DOS should be stretched by 12%, in order to match the experimental cutoff energy; see Fig. 3. Better agreement in the cutoff energy obtained by the provided phonon dispersion relation is found in a report where relativistic corrections and spin-orbit coupling were included [31].

A series of thermodynamic parameters is obtained by weighted integration of the DOS [29]. The recoil-free fraction, known as the Lamb-Mössbauer factor, f_{LM} , for Os at room temperature is $0.95(1)$. Such a high f_{LM} is comparable only with the f_{LM} in Ta using the ^{181}Ta transition at $6.214(2) \text{ keV}$ [35]. The Debye speed of sound, u_D , can be extracted from $\lim_{E \rightarrow 0} \frac{g(E)}{E^2}$. The Debye representation of the DOS is fitted with a zero slope line between 5 and 11 meV, see inset to Fig. 3, and the obtained $\lim_{E \rightarrow 0} \frac{g(E)}{E^2}$ is $5.3(6) \times 10^{-5} \text{ meV}^{-3}$. The extracted Debye speed of sound at room temperature is $u_D = 3.58(14) \text{ km/s}$. The longitudinal, $u_L = 5.747 \text{ km/s}$, and transversal, $u_T = 3.425 \text{ km/s}$, speed of sound measured in a polycrystalline Os-metal sample at 300 K by Pantea *et al.* [36] result in an average Debye speed of sound $u_D = 3.791 \text{ km/s}$, close to the speed of sound extracted herein. The mean force constant for Os is obtained from the second moment of the DOS and is $335(5) \text{ N/m}$. Diamond and osmium have similar bulk moduli [2]. The mean force constant in Os metal is almost half of the interatomic mean force constant of carbon

in diamond, i.e., 775 N/m [37]. This is expected because the covalent bonding in diamond is stronger than the metallic bonding in Os metal.

Os and Fe are isoelectronic in d valence electrons, but, at ambient conditions Fe crystallizes in bcc and Os in the hcp structure. At room temperature under application of 15 GPa bcc (α -Fe) transforms to hcp (ϵ -Fe). The mass ratio between Fe and Os is $(\frac{M_{Fe}}{M_{Os}})^{1/2} = 1/1.81$ and the lattice parameters ratio in the hcp structure is $\frac{a_{Fe}(25\text{GPa})}{a_{Os}} = \frac{c_{Fe}(25\text{GPa})}{c_{Os}} = 1/1.1$. According to the mass homology relation [38] the Fe vibrational modes with energy E_{Fe} should be energy-compressed in order to match the vibrational modes of Os with energy E_{Os} with a compression constant, $\frac{E_{Fe}}{E_{Os}} = 1/(1.81 \times 1.1) = 1/1.99$. Figure 3 shows in addition to the Os DOS obtained herein the ϵ -Fe DOS obtained at 25 GPa by Mao *et al.* [39]. The main features in the DOS of Os are reproduced and thus elastically Os is a model for ϵ -Fe at ambient conditions. In order to match the phonon cutoff energy of Os DOS the energy axis of the ϵ -Fe DOS should be compressed by 1.55. This is $\sim 22\%$ lower compared with the energy compression constant indicated by the mass homology relation. Such a difference might only be explained by a slight difference in bonding between ϵ -Fe and Os. The mean force constant calculated from the DOS in ϵ -Fe at 25 GPa is, 235 N/m, indeed lower than the corresponding in Os.

IV. CONCLUSIONS

In summary, we have studied the nuclear forward and inelastic scattering of synchrotron radiation by the low-lying nuclear level of ^{187}Os in Os metal. We refined the energy

of the transition, 9.778(3) keV, and the lifetime of the first excited state, 3.06(8) ns. In addition, we have determined the previously unknown nuclear quadrupole moment of the first excited state, $Q_{3/2} = 1.46(10)$ b. We carried out nuclear inelastic scattering spectroscopy with a 1-meV resolution and extracted the density of phonon states in Os metal. We provide a basis for refining the Os potential in first-principle theoretical calculations for osmium compounds. We indicate that from a lattice dynamics perspective Os is a model of Fe at high pressure with minor differences in the local environment. As measurements of hyperfine interactions in Os compounds are practically not feasible using both Mössbauer and NMR spectroscopy, we suggest that nuclear forward scattering is a viable promising technique for measuring the hyperfine interactions in Os compounds, including Os organometallics.

ACKNOWLEDGMENTS

J.W. and V.S. acknowledge the support from the German Federal Ministry of Education and Research under 05K13UK2. P.J.S. and R.J.N. acknowledge support from the ERC (Grant No. 247450). R.P.H. acknowledges the Helmholtz Association of German research centers for funding (VH NG-407, “Lattice dynamics in emerging functional materials”). The European Synchrotron Radiation Facility is acknowledged for provision of synchrotron radiation beam time at the Nuclear Resonance beamline ID18. J.-P. Celse, B. Picut, and J.-P. Vassalli are acknowledged for technical assistance during the mechanical construction and the crystal preparation of the dedicated high-resolution monochromator, respectively.

-
- [1] D. R. Lide and H. P. R. Frederikse, *CRC Handbook of Chemistry and Physics* (CRC Press, Boca Raton, FL, 1997).
 - [2] H. Cynn, J. E. Klepeis, C.-S. Yoo, and D. A. Young, *Phys. Rev. Lett.* **88**, 135701 (2002).
 - [3] F. Occelli, D. L. Farber, J. Badro, C. M. Aracne, D. M. Teter, M. Hanfland, B. Canny, and B. Couzinet, *Phys. Rev. Lett.* **93**, 095502 (2004).
 - [4] W. P. Griffith, *Q. Rev. Chem. Soc.* **19**, 254 (1965).
 - [5] L. Ronconi and P. J. Sadler, *Coord. Chem. Rev.* **252**, 2239 (2008).
 - [6] F. Wagner, D. Kucheida, U. Zahn, and G. Kaindl, *Z. Angew. Phys.* **266**, 223 (1974).
 - [7] B. C. Sales, O. Delaire, M. A. McGuire, and A. F. May, *Phys. Rev. B* **83**, 125209 (2011).
 - [8] M. M. Koza, D. Adroja, N. Takeda, Z. Henkie, and T. Cichorek, *J. Phys. Soc. Jpn.* **82**, 114607 (2013).
 - [9] A. K. Paul, M. Reehuis, V. Ksenofontov, B. Yan, A. Hoser, D. M. Többsens, P. M. Abdala, P. Adler, M. Jansen, and C. Felser, *Phys. Rev. Lett.* **111**, 167205 (2013).
 - [10] K. Shimizu, T. Kimura, S. Furomoto, K. Takeda, K. Kontani, Y. Onuki, and K. Amaya, *Nature (London)* **412**, 316 (2001).
 - [11] Y. Ma, M. Somayazulu, G. Shen, H. Kwang Mao, J. Shu, and R. J. Hemley, *Phys. Earth Planet. Inter.* **143-144**, 455 (2004).
 - [12] R. J. Hemley and H.-K. Mao, *Int. Geol. Rev.* **43**, 1 (2001).
 - [13] S. D. Shnyder, Y. Fu, A. Habtemariam, S. H. van Rijt, P. A. Cooper, P. M. Loadman, and P. J. Sadler, *Med. Chem. Commun.* **2**, 666 (2011).
 - [14] J. B. Hastings, D. P. Siddons, U. van Bürcck, R. Hollatz, and U. Bergmann, *Phys. Rev. Lett.* **66**, 770 (1991).
 - [15] U. van Bürcck, D. P. Siddons, J. B. Hastings, U. Bergmann, and R. Hollatz, *Phys. Rev. B* **46**, 6207 (1992).
 - [16] M. Seto, Y. Yoda, S. Kikuta, X. W. Zhang, and M. Ando, *Phys. Rev. Lett.* **74**, 3828 (1995).
 - [17] W. Sturhahn, T. S. Toellner, E. E. Alp, X. Zhang, M. Ando, Y. Yoda, S. Kikuta, M. Seto, C. W. Kimball, and B. Dabrowski, *Phys. Rev. Lett.* **74**, 3832 (1995).
 - [18] M. Basunia, *Nucl. Data Sheets* **110**, 999 (2009).
 - [19] R. Rüffer and A. I. Chumakov, *Hyperfine Interact.* **97-98**, 589 (1996).
 - [20] A. I. Chumakov, I. Sergeev, J.-P. Celse, R. Rüffer, M. Lesourd, L. Zhang, and M. Sánchez del Río, *J. Synchrotron Radiat.* **21**, 315 (2014).
 - [21] A. Baron, *Hyperfine Interact.* **125**, 29 (2000).
 - [22] S. Kraft, J. Stümpel, P. Becker, and U. Kuetgens, *Rev. Sci. Instrum.* **67**, 681 (1996).

- [23] Y. V. Shvyd'ko, M. Lerche, J. Jäschke, M. Lucht, E. Gerdau, M. Gerken, H. D. Rüter, H.-C. Wille, P. Becker, E. E. Alp *et al.*, *Phys. Rev. Lett.* **85**, 495 (2000).
- [24] NIST Physical Reference Data: <http://physics.nist.gov/PhysRefData/contents.html>.
- [25] Y. V. Shvyd'ko, *X-Ray Optics: High Energy-Resolution Applications* (Springer-Verlag, Berlin, Heidelberg, 2004).
- [26] J. Y. Zhao, T. S. Toellner, M. Y. Hu, W. Sturhahn, E. E. Alp, G. Y. Shen, and H. K. Mao, *Rev. Sci. Instrum.* **73**, 1608 (2002).
- [27] M. Yabashi, K. Tamasaku, S. Kikuta, and T. Ishikawa, *Rev. Sci. Instrum.* **72**, 4080 (2001).
- [28] D. Bessas, D. G. Merkel, A. I. Chumakov, R. Rüffer, R. P. Hermann, I. Sergueev, A. Mahmoud, B. Klobes, M. A. McGuire, M. T. Sougrati *et al.*, *Phys. Rev. Lett.* **113**, 147601 (2014).
- [29] V. Kohn and A. Chumakov, *Hyperfine Interact.* **125**, 205 (2000).
- [30] Y. Ma, T. Cui, L. Zhang, Y. Xie, G. Zou, J. S. Tse, X. Gao, and D. D. Klug, *Phys. Rev. B* **72**, 174103 (2005).
- [31] B. Xu and M. J. Verstraete, *Phys. Rev. B* **87**, 134302 (2013).
- [32] Y. Liang and Z. Fang, *J. Phys.: Condens. Matter* **18**, 8749 (2006).
- [33] X. Deng, W. Wang, D. Zhang, and K. You, *Physica B* **406**, 656 (2011).
- [34] C.-M. Liu, Y. Cheng, B. Zhu, and G.-F. Ji, *Physica B* **406**, 2110 (2011).
- [35] A. I. Chumakov, A. Q. R. Baron, J. Arthur, S. L. Ruby, G. S. Brown, G. V. Smirnov, U. van Bürck, and G. Wortmann, *Phys. Rev. Lett.* **75**, 549 (1995).
- [36] C. Pantea, I. Stroe, H. Ledbetter, J. B. Betts, Y. Zhao, L. L. Daemen, H. Cynn, and A. Migliori, *Phys. Rev. B* **80**, 024112 (2009).
- [37] A. Bosak and M. Krisch, *Phys. Rev. B* **72**, 224305 (2005).
- [38] H. R. Schober and W. Petry, *Lattice Vibrations* (Wiley-VCH Verlag GmbH, Weinheim, 2006).
- [39] H. K. Mao, J. Xu, V. V. Struzhkin, J. Shu, R. J. Hemley, W. Sturhahn, M. Y. Hu, E. E. Alp, L. Vocadlo, D. Alfè *et al.*, *Science* **292**, 914 (2001).